Phase transformation of kaolinite to hexagonal kalsilite using K_2CO_3

E. F. Yusslee[1], N. H. Dahon[1], M. A. A. Rajak[1], S. N. S. Bakri[1], S. E. Arshad[2#]*
[1]*Universiti Malaysia Sabah, Preparatory Centre for Science and Technology, 88400 Kota Kinabalu, Malaysia*
[2]*Universiti Malaysia Sabah, Faculty of Science and Natural Resources, 88400 Kota Kinabalu, Malaysia*

Abstract

Hydrothermal synthesis of kalsilite was facilitated by the inclusion of potassium carbonate (K_2CO_3) as the source of the potassium ion. After a 24 h reaction at 220 °C, kaolin clay treated with 1.25 M K_2CO_3 showed the most significant peaks at 2θ of 28.5° and 34.7° by X-ray diffraction corresponding to the hexagonal kalsilite. In addition, field emission scanning electron microscopy images also revealed hexagonal particles proving the formation of the desired mineral. The orthorhombic boehmite and monoclinic bayerite were formed as the dominant phases at lower K_2CO_3 molarity (<1.0 M), whereas kalsilite was recognized as the minor crystalline phase. The crystallinity of hexagonal kalsilite increased at higher K_2CO_3 concentration (>1.0 M) while the reaction temperature remained at 220 °C. Furthermore, the energy dispersive spectroscopy pattern of kalsilite showed a significant atomic percentage of potassium in the aluminosilicate material, indicating its formation.
Keywords: kaolin, crystallization, potassium aluminum silicate, diffraction.

INTRODUCTION

In recent years, research communities have been paying more attention to kaolin clay because of its high alumina and silica content and its wide range of applications, including ceramics, cement, and agriculture[1, 2]. Besides that, the paper, rubber, and plastics industries also use a significant amount of kaolin clay. In kaolin, kaolinite is the most predominant clay component [3]. This mineral has two layers: one layer of $[SiO_4]^{4-}$ tetrahedra and one layer of $[AlO_2(OH)_4]^{5-}$ octahedron [4]. Oxygen bridges connect the tetrahedral and octahedral layers, whereas each oxygen from the bridge is a $[SiO_4]^{4-}$ tetrahedron and two $[AlO_2(OH)_4]^{5-}$ octahedrons [5]. The layer packets are held together by weak hydrogen bonds.

Several studies on kalsilite synthesis using kaolin clay as starting material have been reported [6, 7]. The mineral kalsilite ($KAlSiO_4$) is made primarily of alkaline silicates. Traditional methods for producing kalsilite include condensing an alumina and silica source with an alkali silicate solution at high pH to create the framework, which consists of an unorganized network of tetrahedral Si and Al units, with the presence of alkali metal ions to balance out the charge [8]. Kalsilite can be synthesized from a range of Si and Al sources using a variety of methods [9-11]; however, hydrothermal [12, 13] and solid state [14, 15] methods are inexpensive and relatively straightforward procedures to manufacture pure crystals with smaller particle sizes. The limited scientific literature describes how kaolinite can be converted to kalsilite using hydrothermal synthesis. The current study illustrates the impacts of K_2CO_3 concentrations and reaction temperature on kalsilite synthesis from kaolinite by hydrothermal treatment. It was followed by mineral characterization using X-ray diffraction (XRD) and field emission scanning electron microscopy (FESEM).

MATERIALS AND METHODS

Kaolin (Sibelco) was employed in all synthesis sequences as the primary source of Al_2O_3 and SiO_2. The chemical composition of kaolin is shown in Table I. To reach the necessary ratio, $Al(OH)_3$ was used as an additional source of Al_2O_3. Alkali solution was made from potassium carbonate pellets (Merck) and distilled water. 1.0 g of kaolin was mixed with 100 mL of various K_2CO_3 concentrations ranging from 0.50 to 1.25 M in a Teflon-lined stainless steel hydrothermal reactor and heated at 10 °C/min to 220 °C for 24 h. The reactor's pressure was approximately equal to the water's vapor pressure at the corresponding temperature. After cooling to room temperature, the products were filtered and washed repeatedly using distilled water and dried at 80 °C in an oven for 8 h.

Table I - Main chemical composition (wt%) of kaolin.

Al_2O_3	SiO_2	Fe_2O_3	K_2O	TiO_2	MgO	LOI
34.20	49.60	1.01	1.80	0.55	0.55	12.10

LOI: loss on ignition.

Characterization: the untreated kaolin and minerals formed were characterized using an X-ray diffractometer (Smartlab, Rigaku). Data collection was carried out in the 2θ range of 5° to 80°, step size of 0.01° under CuKα radiation (1.540 Å), 50 mA, and 40 kV. Phase identification was performed by referring to the ICDD (International Centre for

**eddy@ums.edu.my*
https://orcid.org/0000-0002-2346-2190
#*sazmal@ums.edu.my*
https://orcid.org/0000-0002-4169-6994

Diffraction Data) powder diffraction file database, with the help of ICDD PDF4+ 2021 files for inorganic compounds. The relative intensity yields for each phase were calculated using normalized XRD peak intensities of the primary reflection. Scherrer's formula was used to calculate the average crystallite size, D, according to:

$$D = \frac{K.\lambda}{\beta.\cos\theta} \quad (A)$$

where K is a constant, λ is the X-ray wavelength, β is the full width at half maximum (FWHM) of the diffraction peak, and θ is the scattering angle. The morphologies of the platinum-coated samples were investigated using a FESEM microscope (JSM-7900F, Jeol). The sample was coated with a platinum layer to prevent charging effects from free electrons and get a clear image. A conductive element, such as platinum (Pt), discharges the free electron liberated by the electron beam's bombardment of the sample's surface. FESEM magnifications of up to 30000x were used to examine coated materials.

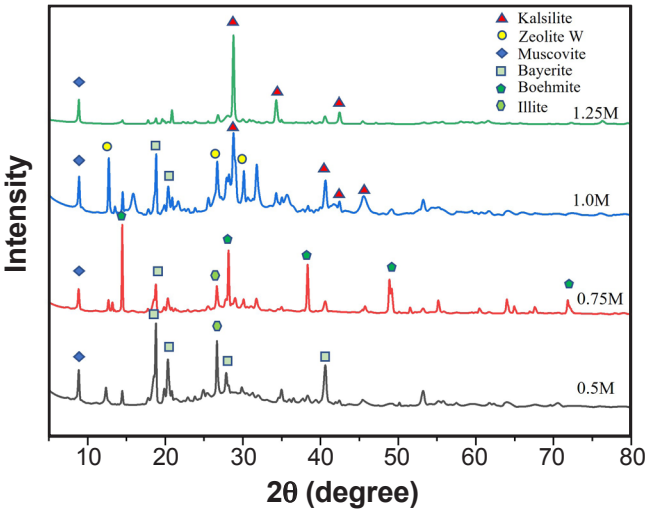

Figure 1: XRD diffractograms of hydrothermal reaction products obtained at various K_2CO_3 concentrations using kaolinite as a precursor at 220 °C for 24 h.

RESULTS AND DISCUSSION

Effect of K_2CO_3 concentrations: formation of kalsilite by using kaolinite as Si and Al source in K_2CO_3 solution can be presented based on the reaction:

$$Al_2Si_2O_5(OH)_4 + K_2CO_3 \rightarrow 2KAlSiO_4 + 2H_2O + CO_2 \quad (B)$$

By referring to the stoichiometry in Eq. B, 2 mols of kalsilite are formed from 1 mol of kaolin and 1 mol of K_2CO_3. Fig. 1 shows XRD diffractograms when kaolin was added with various K_2CO_3 concentrations for the kalsilite formation. From the results, 1.25 M KOH showed the most significant kalsilite peaks (PDF file 00-011-0579) at 28.5° (102), 34.7° (110), and 42.3° (004). High K_2CO_3 concentrations (>1.0 M) were essential to forming kalsilite crystals due to the availability of Si and Al in the reaction medium to interact with the abundance of K^+ ions in the nucleation process, resulting in the formation of $KAlSiO_4$ crystals. This finding is in line with observations found by N'Guessan et al. [16], where faster Si and Al dissolution of kaolin reported occurred at 2 M KOH, which affects the re-precipitation process, hence in this study, leading to the formation of the desired kalsilite. When comparing the results to the findings by Su et al. [17], there was a significant improvement in terms of K^+ concentration and reaction time, where the latter reported using 4.3 M KOH combined with microcline powder from syenite to synthesize $KAlSiO_4$ for 3 h utilizing a hydrothermal reaction technique. In comparison to the previous literature [17], this work demonstrated that kaolin may also be employed as a precursor for kalsilite synthesis via hydrothermal reaction due to its high Si and Al contents. Although the study by Su et al. [17] consumed lower reaction time, which was mainly due to the ready existence of K^+ ion in its precursor's crystal structure, this study used substantially lower K_2CO_3 molarity, which provided a greener alternative of K^+ source for kalsilite formation.

Further reduction in K_2CO_3 concentration, on the other hand, promoted multiple diffraction peaks corresponding to the minerals bayerite (PDF 01-074-1119), boehmite (PDF 01-073-9093), and illite (PDF 00-026-0911). When 1.0 M K_2CO_3 was used in the hydrothermal process, kalsilite crystals formed a minor crystalline phase, with bayerite being the dominating phase. These findings may be a direct consequence of the lower dissolution rate of Si and Al in the reaction medium [16], hence unable to breakdown the monoclinic bayerite crystal as shown in Fig. 2. The existence of several mineral peaks in the diffractograms at lower K_2CO_3 concentration suggested that Si and Al dissolution in kaolin occurred ineffectively due to a lack of K^+ ions, resulting in recrystallization of the precursor creating various forms of minerals [18]. The schematic diagram of the transformation of hexagonal kalsilite from kaolinite can be seen in Fig. 2.

Effect of reaction temperature: the XRD patterns of the products formed at different reaction temperatures are shown in Fig. 3. As can be seen after the reaction at 180 ºC, muscovite existed as the primary phase with the existence of minor peaks for zeolite W, megakalsilite, and kalsilite. This indicated the incorporation of K^+ at the correct 1:1 ratio was unsuccessful, most probably due to limited energy supplied for the transformation of kaolinite lattice structure resulting in metastable intermediate products. The results of this experiment were quite different from the work done by Probst et al. [19], where they reported kalsilite was the major product when kaolin clay reacted with KOH solution at 180 °C. The difference in the formed crystal can be attributed to a number of factors. Firstly, the molarity of KOH used was higher (4.3 M), and secondly, the different elemental composition of the kaolin precursor compared to this study affected the results obtained. On the other hand, the diffraction peaks of muscovite and zeolite W gradually

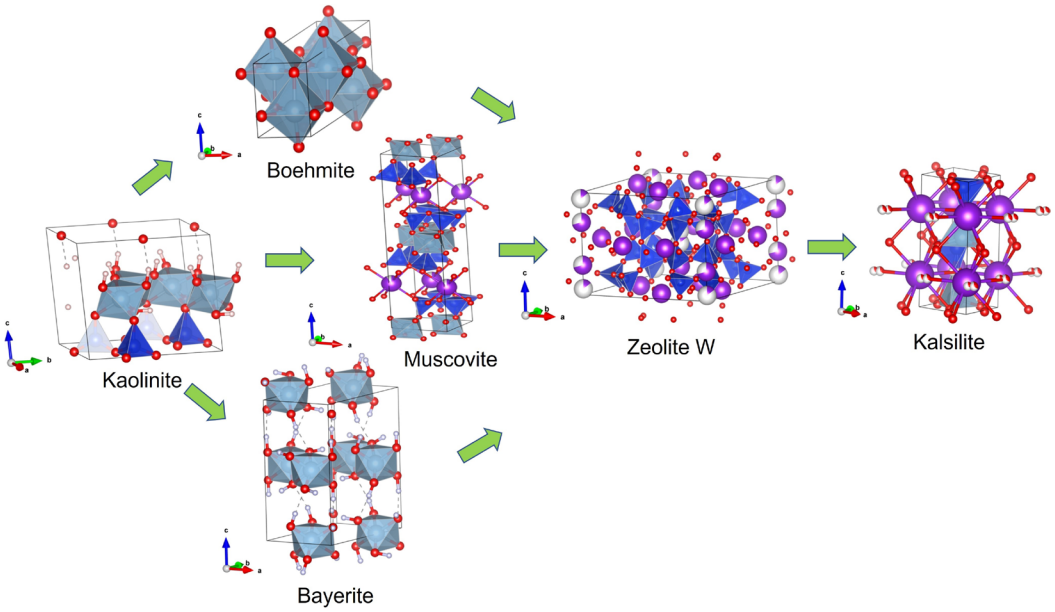

Figure 2: Schematic diagram of the three-dimensional crystal structure transformation from C_1 kaolinite to $P6_3$ hexagonal kalsilite using Vesta software [25] and data obtained from ICDD PDF4+ 2021.

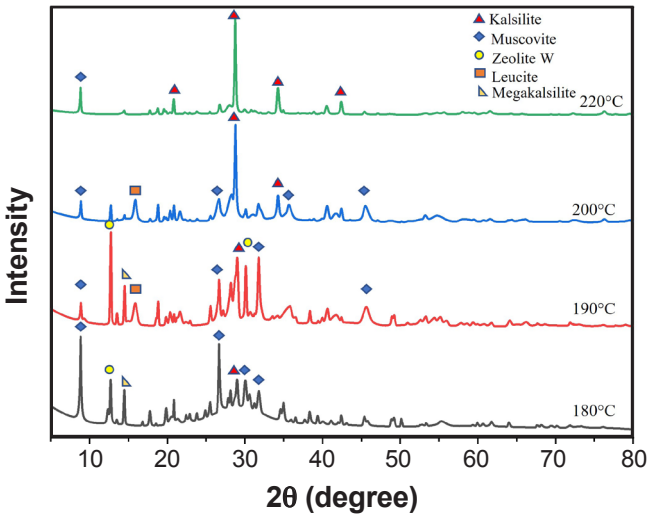

Figure 3: XRD diffractograms of hydrothermal reaction products obtained at various reaction temperatures using kaolinite and 1.25 M K_2CO_3 as precursors for 24 h.

disappeared as the reaction temperature increased up to 220 ºC where two new distinctive peaks at 28.5º (102) and 34.7º (110) were observed, corresponding for hexagonal kalsilite. The results were in contrast with the findings from a previous study reported by Wen and Yan [20] where kalsilite was prepared by calcining dried slurry made of aqueous potassium silicate and potassium hydroxide solutions as well as aqueous aluminum nitrate at 1000 and 1200 ºC. The present hydrothermal method used a temperature almost 5 times lower than the work by Wen and Yan [20] and 4 times lower than the study by Batir et al. [21] to synthesize kalsilite, potentially reducing the production cost. Moreover, the product formed in this work had smaller crystallites, which are highly suitable in the catalysis field.

Morphology analysis by FESEM: morphological characterizations of the raw kaolin and synthesized products are illustrated in Figs. 4 and 5. Fig. 4a shows flake-like material corresponding to raw kaolin as a precursor, while Fig. 4b shows pillar-shaped crystals of metastable phase after the 0.75 M K_2CO_3 was used. The formation of hexagonal kalsilite can be seen in Fig. 4c after raw kaolin was treated with 1.25 M K_2CO_3 at 220 °C. The average crystallite size of $KAlSiO_4$ was 110 nm. The theoretical result was in accordance with the FESEM images showing the average particle size of the crystal around 120 nm. This observation was also supported by findings from Kimura et al. [22], where they obtained tiny crystals of kalsilite at almost the same size (~100 nm) after using nano-sodalite as a precursor for nepheline synthesis. These results demonstrated that raw kaolin can be transformed into kalsilite using a hydrothermal technique while producing nano-size crystals comparable to the solid-state method.

Fig. 5 presents the effect of reaction temperature on the product morphologies. Square-pillar shape and needle-like shape of the metastable phase of zeolite W and muscovite were observed (Fig. 5a) when the reaction was carried out at 190 °C. This clearly demonstrated the consistency with the previous study [23] where an identical elongated structure of zeolite W was observed at 175 °C after being synthesized in a Teflon-lined stainless steel autoclave for 48 h. Further heating the hydrothermal reactor to 220 °C resulted in hexagonal kalsilite (Fig. 5b). The findings of this experiment were compatible with those obtained from Wu et al. [24]; they observed the formation of hexagonal crystal at 220 °C, which is comparable to the temperature of the current study. Fig. 6 shows the results of EDS analyses for raw kaolin and kalsilite formed where a significant increase of potassium (K) atomic percentage in the final product was evidence for the formation of kalsilite.

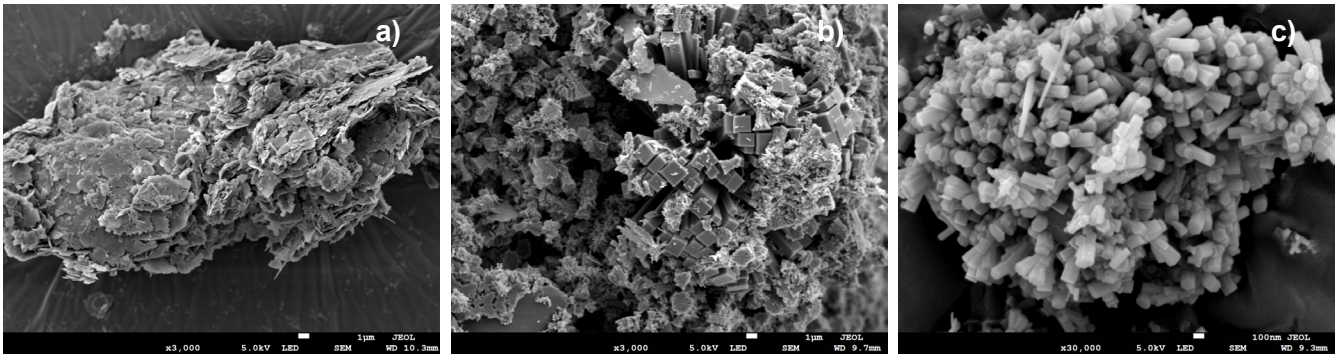

Figure 4: FESEM images of: a) raw kaolin; b) product formed after being treated with 0.75 M K_2CO_3 at 220 °C; and c) kalsilite formed after being treated with 1.25 M K_2CO_3 at 220 °C.

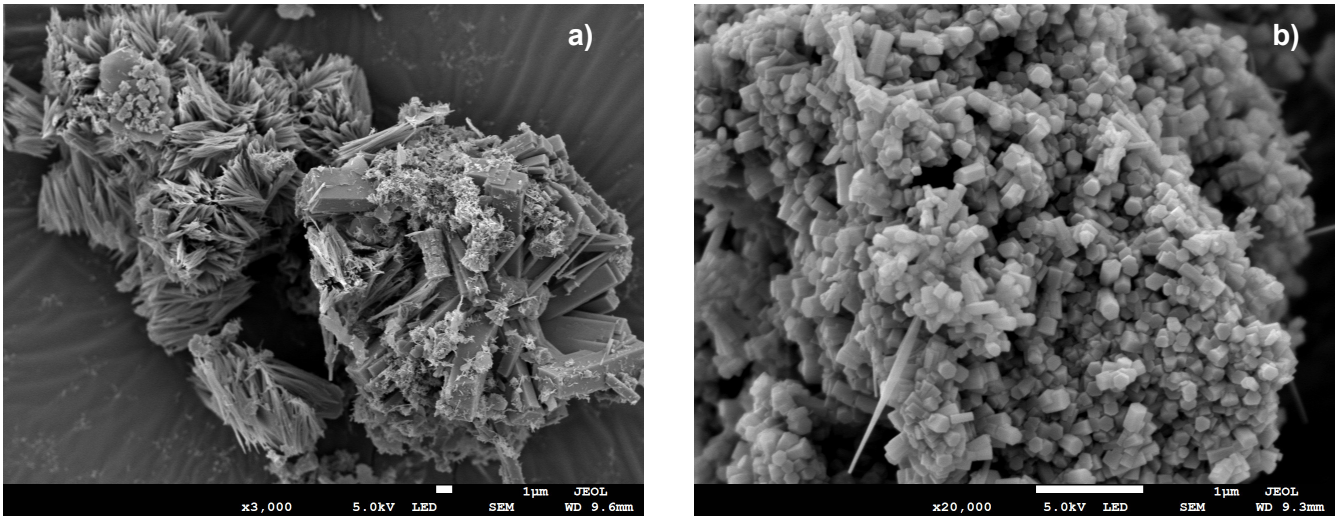

Figure 5: FESEM images of the a) metastable product formed after being treated with 1.25 M K_2CO_3 at 190 °C and b) kalsilite formed after being treated with 1.25 M K_2CO_3 at 220 °C.

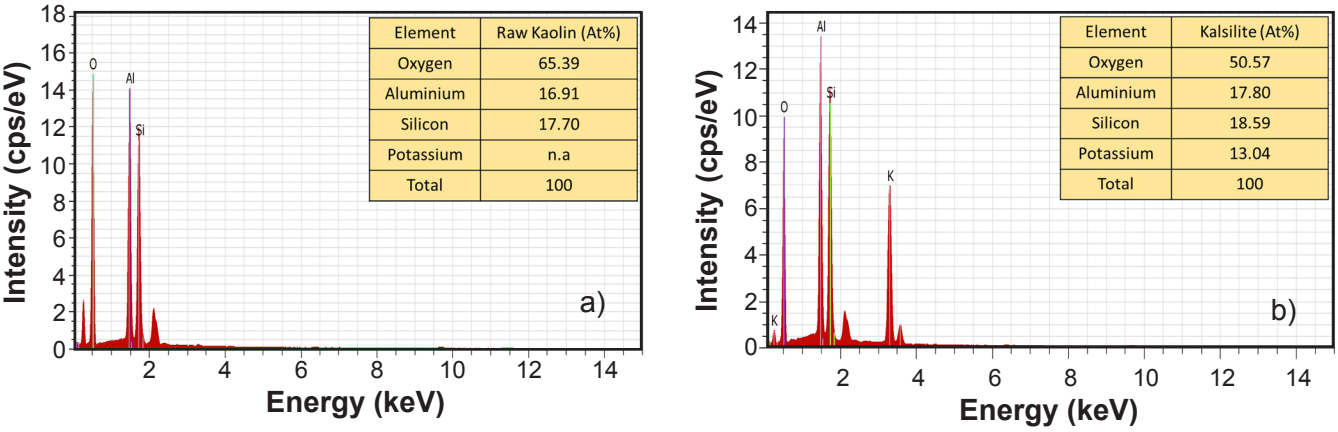

Element	Raw Kaolin (At%)
Oxygen	65.39
Aluminium	16.91
Silicon	17.70
Potassium	n.a
Total	100

Element	Kalsilite (At%)
Oxygen	50.57
Aluminium	17.80
Silicon	18.59
Potassium	13.04
Total	100

Figure 6: Results of EDS analysis of: a) raw kaolin; and b) kalsilite formed at 220 °C.

CONCLUSIONS

Kalsilite was successfully synthesized using kaolin and K_2CO_3 as precursors by hydrothermal technique and the influence of K_2CO_3 concentrations and reaction temperature on crystal formation were investigated. When kaolinite was treated with 1.25 M K_2CO_3 in a hydrothermal method at 220 °C for 24 h, it transformed into kalsilite. High K_2CO_3 concentrations used in the reaction improved the crystallinity of the kalsilite formed. On the other hand, for low K_2CO_3 concentration (<1.25 M), boehmite, muscovite, and bayerite were formed due to the ineffective incorporation of K^+ ions during the recrystallization of precursors. Besides, monoclinic muscovite was the dominant product when the

reaction was carried out at a low temperature (<220 °C). Using Scherrer's equation, the average crystallite size of $KAlSiO_4$ formed was 110 nm. The results were confirmed by XRD diffractograms, EDS graphs, and FESEM images of the products.

ACKNOWLEDGEMENTS

The authors gratefully acknowledge and appreciate the financial supports from Universiti Malaysia Sabah, Malaysia (SBK0412-2018 & GUG0248-2018), and Dr. Melbert Jeem from Hokkaido University for the crystallization interpretation.

REFERENCES

[1] A.S. Hamizah, A.R. Rashita, S. Malek, Mater. Today Proc. **29** (2019) 173.
[2] A.B. Neji, M. Jridi, H. Kchaou, M. Nasri, R. Dhouib Sahnoun, Polym. Test. **84** (2020) 106380.
[3] E.B.G. Johnson, S.E. Arshad, Appl. Clay Sci. **97-98** (2014) 215.
[4] H. Yang, D. Tong, Y. Dong, L. Ren, K. Fang, C. Zhou, W. Yu, Appl. Clay Sci. **188** (2020) 105512.
[5] T. Ondro, A. Trník, AIP Conf. Proc. **1988** (2018) 20033.
[6] C.A.R. Reyes, C.D. Williams, DYNA **77**, 163 (2010) 55.
[7] A.I. Becerro, A. Escudero, M. Mantovani, Am. Mineral. **94**, 11-12 (2009) 1672.
[8] G. Wen, Z. Yan, M. Smith, P. Zhang, B. Wen, Fuel **89**, 8 (2010) 2163.
[9] I. Sobrados, M. Gregorkiewitz, Phys. Chem. Miner. **20**, 6 (1993) 433.
[10] V. Dondur, N. Petranović, R. Dimitrijevic, Mater. Sci. Forum **214** (1996) 91.
[11] P. Kumar, V. Singh, S. Hira, P. Manna, P. Kumar, Int. J. Appl. Ceram. Technol. **13**, 1 (2016) 78.
[12] E.F. Yusslee, N.H. Dahon, M. Azrul, A. Rajak, S.E. Arshad, Malaysian J. Chem. **23**, 2 (2021) 115.
[13] D. Novembre, D. Gimeno, N. d'Alessandro, L. Tonucci, Mineral. Mag. **82**, 4 (2018) 961.
[14] N. Brachhold, C.G. Aneziris, Int. J. Appl. Ceram. Technol. **10**, 4 (2012) 707.
[15] N. Brachhold, C.G. Aneziris, Refract. Worldforum **6** (2014) 93.
[16] N.E. N'Guessan, E. Joussein, A. Courtin-Nomade, E. Paineau, M. Soubrand, O. Grauby, V. Robin, C.D. Cristina, D. Vantelon, P. Launois, P. Fondanèche, S. Rossignol, N. Texier-Mandoki, X. Bourbon, Appl. Clay Sci. **205** (2021) 106037.
[17] S.Q. Su, H.W. Ma, J. Yang, P. Zhang, Z. Luo, Int. J. Miner. Metall. Mater. **21**, 8 (2014) 826.
[18] E.F. Yusslee, N.H. Dahon, M.A. Abd Rajak, S.E. Arshad, Ceram. Silik. **65**, 4 (2021) 363.
[19] J. Probst, J.G. Outram, S.J. Couperthwaite, G.J. Millar, P. Kaparaju, Microporous Mesoporous Mater. **316** (2021) 110918.
[20] G. Wen, Z. Yan, Front. Chem. Sci. Eng. **5**, 3 (2011) 325.
[21] O. Batir, N. Selçuk, G. Kulah, Combust. Sci. Technol. **191**, 1 (2019) 43.
[22] R. Kimura, J. Wakabayashi, S.P. Elangovan, M. Ogura, T. Okubo, J. Am. Chem. Soc. **130**, 39 (2008) 12844.
[23] M. Houlleberghs, E. Breynaert, K. Asselman, E. Vaneeckhaute, S. Radhakrishnan, M.W. Anderson, F. Taulelle, M. Haouas, J.A. Martens, C.E.A. Kirschhock, Microporous Mesoporous Mater. **274** (2019) 379.
[24] Y. Wu, L. Li, X. Liu, Y. Wang, M. Li, Miner. Eng. **178** (2022) 107392.
[25] K. Momma, F. Izumi, J. Appl. Crystallogr. **44**, 6 (2011) 1272.

(Rec. 08/07/2022, Rev. 22/09/2022, Ac. 28/09/2022)